

# Photon creation from vacuum and interactions engineering in nonstationary circuit QED

A V Dodonov

*Departamento de Física, Universidade Federal de São Carlos, 13565-905, São Carlos, SP, Brazil*

We study theoretically the nonstationary circuit QED system in which the artificial atom transition frequency, or the atom-cavity coupling, have a small periodic time modulation, prescribed externally. The system formed by the atom coupled to a single cavity mode is described by the Rabi Hamiltonian. We show that, in the dispersive regime, when the modulation periodicity is tuned to the ‘resonances’, the system dynamics presents the dynamical Casimir effect, resonant Jaynes-Cummings or resonant Anti-Jaynes-Cummings behaviors, and it can be described by the corresponding effective Hamiltonians. In the resonant atom-cavity regime and under the resonant modulation, the dynamics is similar to the one occurring for a stationary two-level atom in a vibrating cavity, and an entangled state with two photons can be created from vacuum. Moreover, we consider the situation in which the atom-cavity coupling, the atomic frequency, or both have a small nonperiodic time modulation, and show that photons can be created from vacuum in the dispersive regime. Therefore, an analog of the dynamical Casimir effect can be simulated in circuit QED, and several photons, as well as entangled states, can be generated from vacuum due to the anti-rotating term in the Rabi Hamiltonian.

PACS numbers: 42.50.-p, 03.65.-w, 37.30.+i, 42.50.Pq, 32.80.Qk

Keywords: Circuit QED, Dynamical Casimir Effect, Rabi Hamiltonian, Anti-Jaynes-Cummings Hamiltonian

## I. INTRODUCTION

Over the last few decades nonstationary processes in cavities have received considerable attention. One such process is the nonstationary or dynamical Casimir Effect (DCE) – in particular, the creation of photons from vacuum, or another initial field state, in cavity whose geometry [1, 2, 3, 4, 5] or material properties [4, 5, 6, 7, 8, 9] have a periodic time dependence, with the modulation frequency close to twice the unperturbed field eigenfrequency. Nowadays, DCE in cavities is a well studied problem, with a variety of theoretical predictions concerning the number and the statistics of created photons, as well as the influence of detuning, dissipation, boundary conditions, geometry and nonperiodicity of the modulation (see [10, 11, 12] for an extensive list of references). To date, DCE has not been observed in laboratory, however several concrete proposals have appeared over the last years [13, 14, 15, 16, 17, 18], with some of them being currently implemented experimentally [19, 20, 21].

The interest in nonstationary processes in cavities reappeared over the last 5 years due to the progress in the field of Cavity Quantum Electrodynamics (cavity QED [22, 23]) in the condensed matter systems, e.g. semiconductor quantum dots [24, 25, 26, 27, 28, 29], polar molecules [30, 31] and superconducting circuits [32, 33, 34] coupled to high- $Q$  resonators, the latest architecture known as *circuit* QED [33, 35]. In cavity QED, the effective 2-level atom is coupled to the field inside the resonator via the dipole interaction, allowing for observation of the light-matter interaction at the level of single photons and single atoms. The new ingredient in the solid state cavity QED, in particular circuit QED, is the possibility of engineering and manipulating the properties of the artificial 2-level atom and the resonator [33, 36, 37], as well as the interaction strength between them [38], either during the fabrication, or *in situ*.

Recently, the strong resonant and the strong dispersive coupling limits between the artificial atom and a single cavity mode were observed experimentally in circuit QED [33, 39] and other solid state architectures [24, 25, 26, 27, 29]. Moreover, the single photon source [40], single artificial-atom maser [41], multiphoton Fock states [42] and interaction between two artificial atoms (qubits) [37, 43] were implemented experimentally, among many other important achievements (see [35] for more references). Besides, the circuit QED architecture benefits from robust readout schemes of the atomic and the resonator states [38, 42, 44, 45, 46, 47, 48], relatively low dissipative losses [39], state preparation techniques [49] and real time manipulation of the atomic transition frequency via electric and magnetic fields [33, 37, 42] or nonresonant microwave fields [43, 48].

Harnessing the tunability of the atomic transition frequency, the authors in [50, 51] proposed an experimental implementation of the Landau-Zener sweeps in circuit QED, when the atomic frequency increases linearly in time. This allows for generation of single photons, as well as cavity-atom entangled states. In a similar direction, the generation of the quantum vacuum radiation by modulating periodically the vacuum Rabi frequency of an intersubband transition in a doped quantum well system embedded in a planar microcavity was considered in [17, 18, 52, 53], and emission of photon pairs was predicted for ‘resonant’ modulation frequencies. A preliminary theoretical study of the feasibility of realizing the dynamical Casimir effect with a quantum flux qubit in superconducting quantum nanocircuits, as

well as the detection of the generated photons, was reported in [54]. On the other hand, the freedom of controlling in real-time the atomic frequency is currently being explored to couple/decouple one or several qubits to/from the cavity mode in order to implement quantum logic operations [37, 43, 48].

In this paper, following the original proposal [55], we study nonstationary processes in the solid state cavity QED, where a single cavity mode is coupled to a single artificial atom whose transition frequency, or atom-cavity coupling, have a small periodic time modulation, prescribed externally. Such a control over the transition frequency, with compatible modulation frequency, can be achieved in circuit QED with present or near-future technology [37, 42, 48]. We show that in the dispersive atom-cavity regime and under the resonance conditions one obtains completely different effective regimes of the atom-field interaction, which can be approximately described by the resonant Anti-Jaynes-Cummings (AJC), resonant Jaynes-Cummings (JC) or the dynamical Casimir effect (DCE) Hamiltonians. Moreover, in the resonant atom-cavity regime, the system dynamics resembles the behavior of the DCE in the vibrating cavity containing a resonant two-level atom, and entangled states with at most two photons can be generated from vacuum.

We also consider the case, in which the atomic frequency, the atom-cavity coupling parameter, or both have a small nonperiodic time modulation, prescribed externally. Namely, we suppose that the modulation is given by the sum of two harmonic functions with different amplitudes and frequencies. We deduce an effective Hamiltonian in the dispersive regime, and show that photon generation from vacuum is possible for fine tuned modulation frequencies.

Thus, we demonstrate the possibility of simulating the DCE in circuit QED using a single nonstationary atom, instead of a macroscopic dielectric medium as in Refs. [6, 7, 8, 9]. As applications, it could be possible to create excitations, either photonic or atomic, from the initial vacuum state  $|g, 0\rangle$ , generate nonclassical states of light and realize transitions between the states  $\{|g, n\rangle, |e, n \pm 1\rangle\}$  in the dispersive regime, where  $|g\rangle$  and  $|e\rangle$  are the atomic ground and excited states, respectively, and  $|n\rangle$  is the Fock state of the cavity field. A related problem was recently studied in [56], where it was suggested that lasing behavior and the creation of a highly non-thermal population of the oscillator, as well as the cooling, could be implemented using an analogous scheme in the near future.

## II. NONSTATIONARY CIRCUIT QED WITH PERIODIC MODULATION

We assume that the atomic transition frequency  $\Omega(t)$  is given by

$$\Omega(t) = \Omega_0 + \varepsilon f_t. \quad (1)$$

Here  $\Omega_0$  denotes the bare atomic frequency,  $\varepsilon$  is a small modulation amplitude,  $\varepsilon \ll \Omega_0$ , and  $f_t$  is an arbitrary periodic function of time, prescribed externally

$$f_t = \sum_{k=0}^{\infty} [s_k \sin k\eta t + c_k \cos k\eta t], \quad (2)$$

where  $\eta$  is the modulation frequency and  $\{s_k, c_k\}$  form a set of coefficients describing the time modulation. The cavity frequency  $\omega$  and the atom-cavity coupling parameter  $g_0$  are constant, so at the charge degeneracy point [38] the system is described by the Rabi Hamiltonian (RH)

$$H = H_0(t) + g_0(a + a^\dagger)(\sigma_+ + \sigma_-), \quad (3)$$

with  $a$  ( $a^\dagger$ ) being the cavity annihilation (creation) operator,  $\sigma_+ = |e\rangle\langle g|$  and  $\sigma_- = |g\rangle\langle e|$ . The free Hamiltonian is

$$H_0(t) = \omega \hat{n} + \frac{\Omega(t)}{2} \sigma_z, \quad (4)$$

where  $\hat{n} = a^\dagger a$  is the photon number operator,  $\sigma_z = |e\rangle\langle e| - |g\rangle\langle g|$  and we assume  $\hbar = 1$ . In the stationary case,  $\varepsilon = 0$ , one can perform the Rotating Wave Approximation (RWA) and obtain the standard Jaynes-Cummings (JC) Hamiltonian [57], which has been verified in several experiments over the last few years [33, 39, 58, 59, 60]. However, in the nonstationary case, as well as under strong dephasing noise [61], the anti-rotating term ( $a\sigma_- + a^\dagger\sigma_+$ ) cannot always be eliminated. Moreover, it is responsible for producing an analog of the DCE and creating photonic and atomic excitations from vacuum under modulation ‘resonance’ conditions, as shown below.

In the interaction picture with respect to  $H_0(t)$  the interaction Hamiltonian reads

$$H_I = g_0 (e^{i\Xi_-} a \sigma_+ + e^{i\Xi_+} a^\dagger \sigma_+ + h.c.), \quad (5)$$

where h.c. stands for the Hermitian conjugate and

$$\Xi_{\pm} \equiv \int_0^t d\tau [\Omega(\tau) \pm \omega]. \quad (6)$$

All the information about the influence of the external modulation on the system dynamics is contained in the time-dependent coefficients  $\exp(i\Xi_{\pm})$ , which can be significantly simplified by tuning the modulation frequency  $\eta$  to the ‘resonances’. We have explicitly

$$g_0 e^{i\Xi_{\pm}} = g e^{i\Delta_{\pm} t} \sum_{l=0}^{\infty} \frac{1}{l!} \left[ \frac{\varepsilon}{\eta} \sum_{k=1}^{\infty} (\Lambda_k e^{-ik\eta t} - \Lambda_k^* e^{ik\eta t}) \right]^l, \quad (7)$$

where we defined the complex coupling constant

$$g \equiv g_0 \exp \left[ i \frac{\varepsilon}{\eta} \sum_{k=1}^{\infty} k^{-1} s_k \right] \quad (8)$$

and parameters

$$\Lambda_k \equiv -\frac{c_k + i s_k}{2k} \quad (9)$$

$$\Delta_{\pm} \equiv (\Omega_0 + \varepsilon c_0) \pm \omega. \quad (10)$$

### III. ANTI-JAYNES-CUMMINGS (AJC) RESONANCE

The ‘Anti-Jaynes-Cummings’ (AJC) resonance occurs for

$$\eta = \eta_{AJC} \equiv \Delta_+ - \xi, \quad (11)$$

where  $|\xi| \ll \Delta_+$  is a small ‘resonance shift’ to be adjusted afterwards. Assuming a reasonable experimental condition  $\varepsilon/\eta \ll 1$ , we expand  $g_0 \exp(i\Xi_{\pm})$  in (5) to the first order in  $\varepsilon/\eta$  and make RWA, obtaining

$$H_I \simeq g (\theta e^{i\xi t} a^\dagger \sigma_+ + e^{i\Delta_- t} a \sigma_+) + h.c., \quad (12)$$

where the modulation induced dimensionless coupling is

$$\theta \equiv \Lambda_1 \frac{\varepsilon}{\eta}. \quad (13)$$

#### A. Dispersive regime

In the dispersive regime,  $g_0 \sqrt{\langle \hat{n} \rangle} / |\Delta_-| \ll 1$ , where  $\langle \hat{n} \rangle$  is the mean photon number, the Hamiltonian (12) can be approximated by [57]

$$H_I^{(1)} \simeq (g\theta e^{i\xi t} a^\dagger \sigma_+ + h.c.) + \delta (\hat{n} + 1/2) \sigma_z, \quad (14)$$

where

$$\delta = \delta_0 + \mathcal{O}(g_0^2/\Delta_+) \quad (15)$$

and

$$\delta_0 = \frac{g_0^2}{\Delta_-} \quad (16)$$

is the standard dispersive shift [57]. After the unitary time-dependent transformation defined by the operator

$$U = \exp [i\xi t \sigma_z / 2] \quad (17)$$

we get the effective AJC Hamiltonian

$$H_{AJC} = U^{-1} H_I^{(1)} U - i U^{-1} \frac{\partial U}{\partial t} \simeq \frac{\xi + \delta (1 + 2\hat{n})}{2} \sigma_z + (g\theta a^\dagger \sigma_+ + h.c.). \quad (18)$$

For the field initially in the Fock state, by adjusting the resonance shift  $\xi$  in order to make  $|\xi + \delta(1 + 2\hat{n})|$  small compared to  $|g\theta|$ , one obtains approximately the resonant AJC Hamiltonian

$$H_{AJC}^{(r)} \simeq g\theta a^\dagger \sigma_+ + g^* \theta^* a \sigma_- . \quad (19)$$

From the physical point of view, the external modulation supplies the energy  $\omega + \Omega_0$  necessary to create one photon and one atomic excitation simultaneously. Thus, one can create the superposition of states  $|e, 1\rangle$  and  $|g, 0\rangle$  starting from the initial vacuum state  $|g, 0\rangle$  and fine tuning the resonance shift.

In figure 1 we show the exact dynamics for the AJC resonance, obtained through the numerical integration of the Schrödinger equation with the initial Hamiltonian (3), setting the experimental circuit QED parameters  $\Omega_0/\omega = 1.4$ ,  $g_0/\omega = 2 \cdot 10^{-2}$  and assuming  $\varepsilon/\omega = 0.2$ . In all the simulations throughout this paper we consider the harmonic modulation,  $f_t = \sin \eta t$ . In the figure 1a we plot the number of created photons

$$N \equiv \langle \hat{n} \rangle - n_0, \quad (20)$$

for the initial Fock state  $|g, n_0\rangle$  as function of the dimensionless time  $|\theta|g_0t$ , assuming the resonance shift  $\xi = -2\delta_0(1 + n_0)$ . In figure 1b we plot the atom excitation probability  $P_e$ . From figures 1a and 1b one can observe the simultaneous generation of one photon and one atomic excitation, in agreement with the effective AJC Hamiltonian (18). However, the maximal mean number of created photons is slightly less than 1 and depends on the initial photon number  $n_0$ , meaning that the resonance shift was not adjusted precisely. In figure 1c we plot  $N$  for the initial number state  $|g, n_0 = 5\rangle$  for different resonance shifts  $\xi = -2\delta_0(1 + n_0 + x)$ ,  $x = 0, 1, 2, 3, 4$ , demonstrating that it is possible to find an optimum  $\xi$  which reproduces the resonant AJC Hamiltonian and allows for the creation of one photon and the atomic excitation simultaneously.

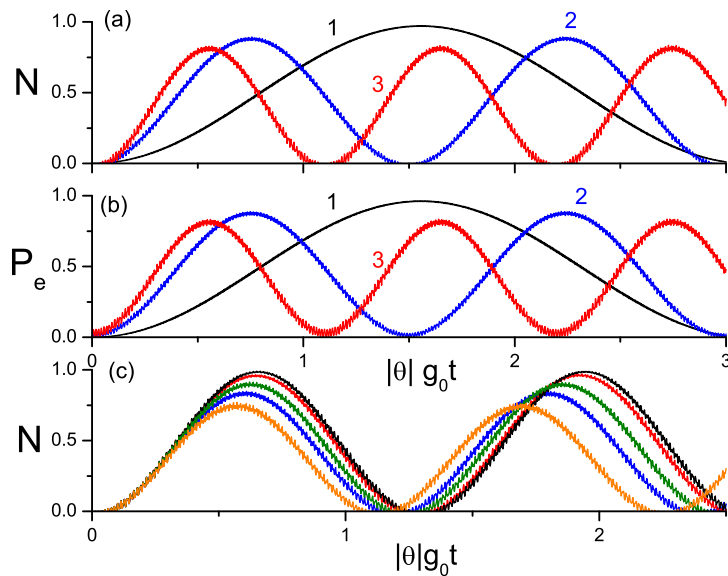


FIG. 1: The results of the numerical integration of the Schrödinger equation with the Rabi Hamiltonian (3) for the modulation frequency  $\eta = \Delta_+ + 2\delta_0(1 + n_0)$ . We see an AJC behavior, as given by the effective Hamiltonian (18). **a)** The number of created photons  $N$  and **b)** the atom excitation probability  $P_e$  versus the dimensionless time for the initial Fock states  $|g, n_0\rangle$ , with  $n_0 = 0$  (line 1),  $n_0 = 3$  (line 2) and  $n_0 = 6$  (line 3). **c)** The dependence of  $N$  on the small change  $x$  in the resonance shift  $\xi = -\delta(1 + n_0 + x)$  for the initial number state  $|g, n_0 = 5\rangle$ . For  $|\theta|g_0t$  from 2 to 2.3 the curves correspond to  $x = 4, 0, 3, 1, 2$ , from below. By adjusting  $x$  one can optimize the photon generation process.

## B. Resonant regime

In the resonant regime,  $|\Delta_-|/g_0 \ll 1$ , the effective Hamiltonian method is not applicable. So we apply the method of slowly varying amplitudes on the Hamiltonian (12), repeating the procedure [62] employed originally for studying

the photon generation from vacuum due to the DCE in a vibrating cavity containing a resonant (stationary) two-level atom [63, 64, 65]. We find that for the initial state  $|g, 0\rangle$  the photon generation occurs for two possible resonance shifts

$$\xi_{\pm} = \Delta_-/2 \pm \sqrt{2}g_0 \quad (21)$$

and one gets the following non-zero probabilities  $P_{an}$ , with  $a = (e, g)$  denoting the atomic state and  $n$  the photon number

$$\begin{aligned} P_{g0} &\approx \cos^2(\chi t) \\ P_{e1} &\approx \sin^2(y+q) \sin^2(\chi t) \\ P_{g2} &\approx \cos^2(y-q) \sin^2(\chi t). \end{aligned} \quad (22)$$

Here

$$\chi \approx |g\theta| \sin(y+q), \quad \tan y \approx \left( \frac{2\sqrt{2}g_0 + \Delta_-}{2\sqrt{2}g_0 - \Delta_-} \right)^{1/2} \quad (23)$$

and  $q = 0$  ( $\pi/2$ ) for  $\xi_-$  ( $\xi_+$ ).

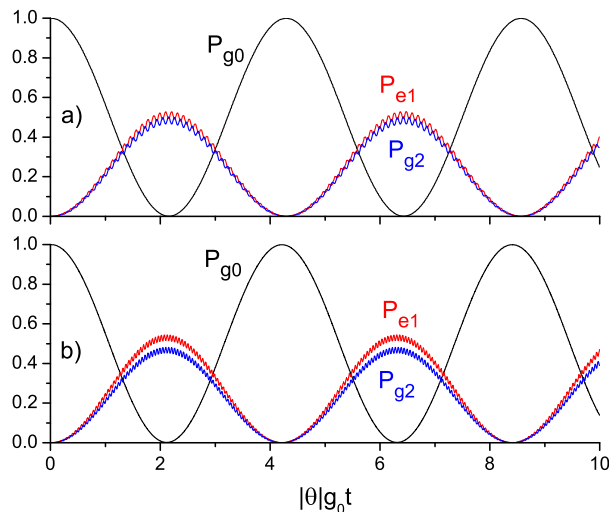


FIG. 2: The time dependence of the probabilities  $P_{g0}$ ,  $P_{e1}$  and  $P_{g2}$ , obtained by the numerical integration of the Schrödinger equation with the Rabi Hamiltonian (3) in the resonant atom-cavity regime for the AJC resonance with properly adjusted frequency shift. **a)**  $\Delta_- = 0$ ,  $\xi = \xi_-$  and  $\varepsilon/\omega_r = 2 \cdot 10^{-1}$ . **b)**  $\Delta_- = 10^{-1}g_0$ ,  $\xi = \xi_-$  and  $\varepsilon/\omega_r = 10^{-1}$ . Not more than 2 photons can be generated from vacuum, and the atom excitation probability is limited by the value  $\sim 1/2$ , in agreement with equation (22).

We illustrate this behavior in figure 2, where we show  $P_{g0}$ ,  $P_{e1}$  and  $P_{g2}$  in the resonant atom-cavity regime under the AJC resonance. In figure 2a we consider  $\Delta_- = 0$  and  $\xi = \xi_-$ , using the parameters  $g_0/\omega = 4 \cdot 10^{-2}$  and  $\varepsilon/\omega = 2 \cdot 10^{-1}$ . In figure 2b we set  $\Delta_- = 10^{-1}g_0$ ,  $\xi = \xi_-$ ,  $g_0/\omega = 4 \cdot 10^{-2}$  and  $\varepsilon/\omega = 10^{-1}$ . The results are in excellent agreement with the theoretical predictions, equation (22), demonstrating that a superposition of states  $|g, 0\rangle$ ,  $|e, 1\rangle$  and  $|g, 2\rangle$  is created from the initial vacuum state  $|g, 0\rangle$ . This dynamics is similar to the one studied in the context of DCE, where a resonant (stationary) two-level atom is fixed inside a cavity whose boundary is oscillating with the frequency close to  $2\omega$  [62]. In both cases not more than two photons can be created from the vacuum state  $|g, 0\rangle$  and the probability of exciting the atom is limited by the value  $1/2$ . This similarity is not surprising, because for the AJC resonance the modulation frequency is  $\eta \approx \Delta_+ \approx 2\omega$ , and the artificial atom plays the role of the stationary two-level atom and the cavity modulating mechanism at the same time.

#### IV. JAYNES-CUMMINGS (JC) RESONANCE

In the dispersive regime the ‘Jaynes-Cummings’ (JC) resonance occurs for

$$\eta = \eta_{JC} \equiv |\Delta_-| - \xi. \quad (24)$$

For  $\Delta_- > 0$ , repeating the steps that led us to (18), we get the effective JC Hamiltonian

$$H_{JC} \simeq \frac{\xi + \delta(1 + 2\hat{n})}{2} \sigma_z + (g\theta a\sigma_+ + h.c.). \quad (25)$$

If  $\Delta_- < 0$ , we obtain (25) upon the replacements  $\theta \rightarrow -\theta^*$  and  $\xi \rightarrow -\xi$ . Thus, by employing the JC resonance and adjusting the resonance shift  $\xi$ , one can couple the subspaces  $\{|g, n\rangle, |e, n-1\rangle\}$  when the atom and the field are far off resonant, since the external modulation supplies the energy difference  $|\Omega_0 - \omega|$  necessary to couple the atom and the cavity field.

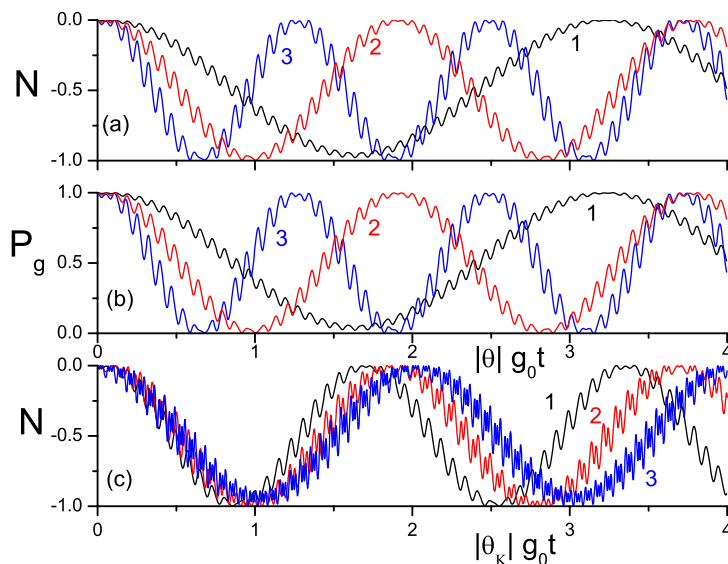


FIG. 3: The results of the numerical integration of the Schrödinger equation with the Rabi Hamiltonian (3) for the JC resonance,  $\eta = \Delta_- + 2\delta_0(1 + n_0)$ , considering initial number states  $|g, n_0\rangle$  with  $n_0 = 1$  (line 1),  $n_0 = 3$  (line 2) and  $n_0 = 7$  (line 3). **a)** The number of created photons  $N$  and **b)** the probability of finding the atom in the ground state  $P_g$  as functions of the dimensionless time demonstrate a transfer between the states  $|g, n_0\rangle$  and  $|e, n_0 - 1\rangle$  in the dispersive regime. **c)**  $N$  for the initial number state  $|g, 4\rangle$  and three lower JC resonances ( $\eta = \eta_-^{(K)}$ ,  $K = 1, 2, 3$  as shown, see section VI) for the resonance shift  $\xi = -10\delta_0$ .

The JC behavior is illustrated in figure 3 for the initial Fock state  $|g, n_0\rangle$ . In figures 3a and 3b we plot  $N$  and  $P_g = 1 - P_e$ , respectively, using the same parameters as in figure 1 and setting  $\eta = \Delta_- + 2\delta_0(1 + n_0)$ . As expected from the effective JC Hamiltonian (25) one has transitions between the states  $\{|g, n\rangle, |e, n-1\rangle\}$  for large detuning,  $|\Delta_-| \gg g$ . Thus, in the dispersive regime one could engineer entangled states with several photons from the initial vacuum state  $|g, 0\rangle$  by alternating between the AJC and JC resonances and controlling the time interval of each resonance.

#### V. DYNAMICAL CASIMIR EFFECT (DCE) RESONANCE

In the dispersive regime, the ‘dynamical Casimir effect’ (DCE) resonance occurs for

$$\eta = \eta_{DCE} \equiv \Delta_+ - \Delta_- - 2\xi = 2\omega - 2\xi. \quad (26)$$

Performing RWA in the interaction Hamiltonian (5) we obtain to the first order in  $\varepsilon/\eta$

$$H_I \simeq g e^{i\Delta_- t} a \sigma_+ + g \theta e^{i(\Delta_- + 2\xi)t} a^\dagger \sigma_+ + h.c. \quad (27)$$

Applying the unitary time-dependent transformation defined by the operator

$$U_1 = \exp \{i [\xi \hat{n} + (\Delta_- + \xi) \sigma_z / 2] t\}, \quad (28)$$

we obtain the time-independent Hamiltonian consisting of the JC Hamiltonian plus the anti-rotating term multiplied by the adjustable coupling  $g\theta$

$$H_I^{(1)} \simeq \xi \hat{n} + \frac{\Delta_- + \xi}{2} \sigma_z + (g a \sigma_+ + g \theta a^\dagger \sigma_+ + h.c.) . \quad (29)$$

Since  $|g/\Delta_-| \ll 1$ , we can obtain an effective Hamiltonian by applying a sequence of small unitary transformations on  $H_I^{(1)}$  [66] and performing the Hausdorff expansion in some small parameter at each step. Here our expansion parameter is  $\epsilon = |g/\Delta_-|$  and, assuming that  $\theta \sim \mathcal{O}(\epsilon)$ , we consider terms up to the second order in  $\epsilon$ . Applying first the ‘rotating’ unitary transformation defined by the time-independent operator

$$U_r = \exp [(g a \sigma_+ - h.c.) / \Delta_-] \quad (30)$$

followed by the ‘antirotating’ transformation defined by the operator

$$U_a = \exp [(g \theta a^\dagger \sigma_+ - h.c.) / (\Delta_- + 2\xi)] , \quad (31)$$

we obtain the effective Hamiltonian

$$H_{eff} = U_a U_r H_I^{(1)} U_r^\dagger U_a^\dagger \quad (32)$$

of the following form (considering terms up to the second order in  $\epsilon$ )

$$H_{eff} \simeq (\xi + \delta \sigma_z) \hat{n} + \delta \sigma_z (\theta^* a^2 + h.c.) + \frac{\Delta_- + \delta + \xi}{2} \sigma_z - \frac{2\delta}{\Delta_-} (g a \hat{n} \sigma_+ + h.c.) + \mathcal{O}(\epsilon^3). \quad (33)$$

Finally, moving to a rotating frame by means of the unitary time-dependent transformation defined by the operator

$$U_2 = \exp [-i (\Delta_- + \delta + \xi) \sigma_z t / 2], \quad (34)$$

we obtain

$$H_{DCE} \simeq (\xi + \delta \sigma_z) \hat{n} + \delta \sigma_z (\theta a^{\dagger 2} + \theta^* a^2) - \frac{2\delta}{\Delta_-} (g e^{i\Delta_- t} a \hat{n} \sigma_+ + h.c.) + \mathcal{O}(\epsilon^3), \quad (35)$$

where we neglected  $(\delta + \xi)$  compared to  $\Delta_-$  in the exponential of the third term.

This is the main result of this section. The first two terms of the effective Hamiltonian (35) form the DCE part and the remaining terms represent corrections, oscillating with a high frequency  $\sim \Delta_-$ . For small  $\langle \hat{n} \rangle \ll n_c \sim (\Delta_-/g)^2$ , the contribution of these corrections is relatively small and  $\sigma_z$  becomes approximately a constant. Assuming that initially the atom is in the ground state, then for  $\langle \hat{n} \rangle \ll n_c$  one has  $\sigma_z \approx -1$  and the right-hand side of equation (35) transforms into the DCE Hamiltonian [4, 5, 11]

$$H_{DCE} \simeq (\xi - \delta) \hat{n} - \delta (\theta a^{\dagger 2} + \theta^* a^2). \quad (36)$$

If the atom is initially in the excited state, a similar effective Hamiltonian is obtained through the substitution  $\delta \rightarrow -\delta$ . Therefore, by adjusting the frequency shift to  $\xi = \pm\delta$ , depending on the initial atomic state [68], we have photon pairs creation from vacuum, as well as field amplification, due to an analog of the DCE.

In this case the DCE is simulated by the atomic transition frequency modulation through the strong atom-cavity coupling. However, the photon generation process is not steady because after several photons have been created the third and higher order terms become important and the photon generation is interrupted. Indeed, the third term describes the non-resonant atomic excitation by means of the absorption of photons from the cavity. Nevertheless, the Hamiltonian (35) shows that it is possible to simulate DCE and generate several photons from vacuum using a single artificial atom.

### A. Qualitative explanation and numerical results

This phenomenon can be qualitatively understood as follows. In the dispersive regime the atom acts as an effective nonlinear capacitance [38], pulling the cavity frequency to approximately

$$\omega(t) \approx \omega + \frac{\sigma_z g_0^2}{\Delta_- + \varepsilon f_t} \approx (\omega + \sigma_z \delta) - \sigma_z \delta \frac{\varepsilon}{\Delta_-} f_t. \quad (37)$$

Consequently, it is expected that the periodic modulation of  $f_t$  with the modulation frequency close to  $\eta \approx 2(\omega \pm \delta)$  will lead to DCE [11, 62], for which the photons are generated as long as the modulation is present. The energy  $2\omega$  necessary to create pairs of photons is provided through the atomic frequency modulation and the resonance shift  $\xi$  must be adjusted [69] in order to get the constructive interference on the cavity field [11, 12]. However, in our case the atom gets entangled with the field due to the third term in (35), by which the atom acquires some probability of being excited through photon absorption and the photon generation process cannot continue asymptotically due to the loss of constructive interference [the first term in (35) becomes non-zero]. This is different from the usual DCE situation, in which the properties of the macroscopic linear, lossless and non-dispersive dielectric medium inside the cavity are modulated [6, 7, 8, 9] and the field mode does not get entangled with individual atoms.

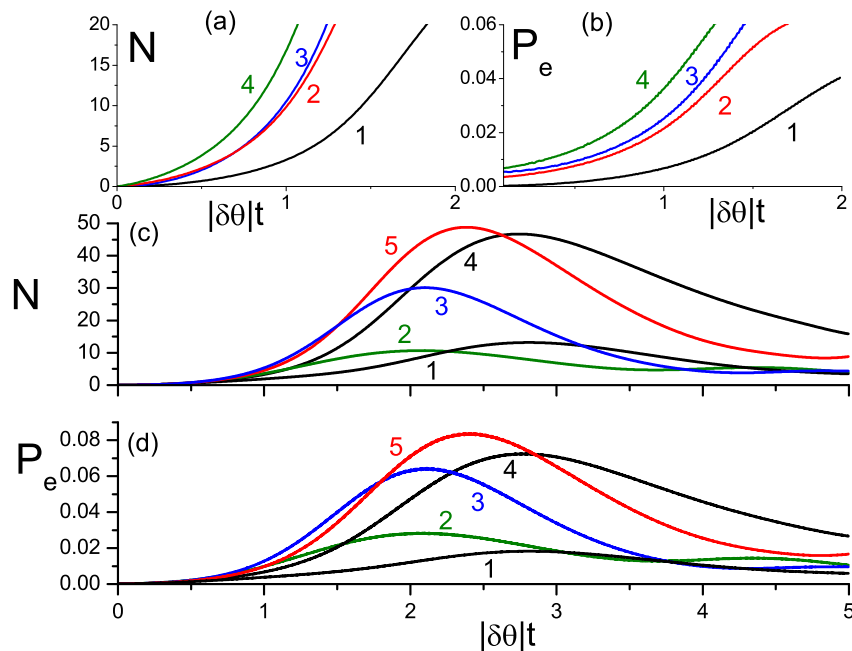


FIG. 4: The initial stage of the time evolution of **a)** the number of created photons  $N$  and **b)** the atom excitation probability  $P_e$ , obtained by the numerical integration of the Schrödinger equation with the Rabi Hamiltonian (3) for  $\eta = 2(\omega_r - \delta_0)$ , for the initial Fock states  $|g, n_0\rangle$  with  $n_0 = 0$  (line 1),  $n_0 = 1$  (line 2) and coherent states  $|g, \alpha\rangle$  with  $|\alpha|^2 = 1/2$  (line 3) and  $|\alpha|^2 = 1$  (line 4). There is photon creation due to an analog of the dynamical Casimir effect, as described by the first two terms in the effective Hamiltonian (35). **c)**  $N$  and **d)**  $P_e$  for larger times and initial state  $|g, 0\rangle$ . Here  $\eta = 2(\omega_r - x\delta_0)$  with  $x = 0.95$  (line 1),  $x = 1.25$  (line 2),  $x = 1.15$  (line 3),  $x = 1$  (line 4) and  $x = 1.05$  (line 5). The photon creation is very sensitive to the resonance shift, and the generation process is interrupted due to the atom-field entanglement, as expected from the third term in equation (35).

In figure 4 we present the results of numerical integration of the Schrödinger equation with the Rabi Hamiltonian (3) for the DCE resonance with properly adjusted frequency shift,  $\eta = 2(\omega - \delta_0)$ , using the parameters  $\Omega_0/\omega = 1.4$ ,  $g_0/\omega = 2 \cdot 10^{-2}$ ,  $\varepsilon/\omega = 4 \cdot 10^{-1}$ . We show the number of created photons  $N$  (figure 4a) and the atom excitation probability  $P_e$  (figure 4b, where the fast oscillations have been averaged out) versus the dimensionless time  $|\delta\theta|t$  for the initial ground atomic state  $|g\rangle$  and the field number states  $|n_0\rangle$  ( $n_0 = 0, 1$ ) and coherent states  $|g, \alpha\rangle$  ( $|\alpha|^2 = 1/2, 1$ ).

For initial times, while  $\langle \hat{n} \rangle \ll n_c \sim 400$ , there is photon generation and amplification, as expected. However, the atom gets entangled with the field and  $P_e$  grows as time goes on, suffering fast oscillations (not shown for clarity), as expected from equation (35).

In figures 4c and 4d we show  $N$  and  $P_e$ , respectively, for larger times and different resonance shifts  $\xi = x\delta_0$ ,  $x = \{0.95, 1, 1.05, 1.15, 1.25\}$ , considering the initial state  $|g, 0\rangle$ . In the first place, we see that the photon generation is very sensitive to the resonance shift in the vicinity of  $\xi = \delta$ , and near the ‘resonance’,  $x \approx 1$ , there is a substantial photon creation from vacuum. However, the photon generation process ceases after several photons have been created and the photon number decreases, although the photon generation process restarts afterwards (data not shown).  $P_e$  resembles the behavior of  $N$ , but remains small for all the times. We also verified numerically that similar results are obtained for different atomic initial states, in agreement with equation (35). Therefore, for  $\eta = 2(\omega \pm \delta)$  one obtains photon generation from vacuum, as well as photon number amplification, analogously to the dynamical Casimir effect [11].

## VI. DISCUSSION OF RESULTS FOR PERIODIC MODULATION

In previous sections we have considered only the first order resonances. In general, the  $K$ -th order resonances occurs for an integer  $K$  when

$$\eta = \eta_i^{(K)} \equiv K^{-1}\eta_i, \quad (38)$$

where  $\eta_i$  stands for the AJC, JC and DCE resonances. In this case one recovers the previous results upon substitutions

$$\delta \rightarrow \delta_K \quad \text{and} \quad \theta \rightarrow \theta_K, \quad (39)$$

as can be deduced from equations (5) and (7). For instance, to obtain  $\theta_K$ , one expands both sums on right-hand side of equation (7) and make RWA, keeping the terms which oscillate with the lowest frequency  $\xi$ . So  $\theta_K$  contains contributions due to the non-harmonic shape of the modulation (e.g.  $\Lambda_K \varepsilon/\eta$ ), as well as due to the powers of  $(\varepsilon/\eta)$  [e.g.  $(\Lambda_1 \varepsilon/\eta)^K / K!$ ]. The effective dispersive shift  $\delta_K$  is obtained analogously, by first performing RWA in (7) and keeping terms which oscillate with frequencies higher than  $\xi$ , and then calculating the effective Hamiltonian, as in equations (14) and (15). So  $\delta_K$  contains the contribution of many terms besides  $\delta_0$ , among them the Bloch-Ziegert shift  $g^2/\Delta_+$  [66] and powers of  $(\varepsilon/\eta)$ . As an example, in figure 3c we show  $N$  versus  $|\theta_K|g_0t$  for the initial number state  $|g, 4\rangle$  and the first three JC resonances, considering the resonance shift  $\xi = -10\delta_0$ . This example illustrates that higher order resonances are readily accessible. However, for the higher order resonances the effective dispersive shift  $\delta_K$  should be carefully evaluated either numerically or experimentally, otherwise there is a risk of missing the exact resonance, since  $|\theta_K|$  becomes smaller and there is less freedom in committing small errors in the resonance shift  $\xi$ .

Our results can be directly transposed to the situation where  $\Omega(t) = \Omega$  is constant and  $g_0 = g_0(t)$  has a periodic time modulation,

$$g_0(t) = g_0 + \varepsilon f_t. \quad (40)$$

In this case, in the interaction picture the interaction Hamiltonian is

$$H_I = \left[ (g_0 + \varepsilon c_0) - \varepsilon \sum_{k=1}^{\infty} k (\Lambda_k^* e^{ik\eta t} + \Lambda_k e^{-ik\eta t}) \right] \left( e^{i(\Omega-\omega)t} a \sigma_+ + e^{i(\Omega+\omega)t} a^\dagger \sigma_+ + h.c. \right). \quad (41)$$

If one expands  $\exp(i\Xi_\pm)$  in equation (7) up to the first order in  $\varepsilon/\eta$ , Hamiltonian (5) becomes equivalent to Hamiltonian (41), so the results obtained above for  $\Omega(t)$  also hold for  $g_0(t)$  after making appropriate substitutions. The main difference between these two cases is that in the  $\Omega(t)$  case the higher order  $K$ -th resonances occur both due to the powers of  $\varepsilon/\eta$  and non-zero coefficients  $\Lambda_K$ , while in the  $g_0(t)$  case the higher order resonances are due only to non-zero coefficients  $\Lambda_K$ . Therefore, for a harmonic modulation,  $f_t = \sin \eta t$ , in the  $\Omega(t)$  case one has higher order resonances, but in the  $g_0(t)$  case there are only the first order resonances. Finally, if the cavity frequency  $\omega$  is modulated periodically, with constant  $\Omega$  and  $g_0$ , the AJC and JC resonances also occur, besides the well known DCE resonance [62, 63, 64, 65].

An experimental verification of this scheme seems possible in circuit QED architecture with superconducting qubits and coplanar waveguide resonators [38], where one can adjust the system parameters *in situ* via electric and magnetic fields, as demonstrated in several experiments [33, 37, 43]. Moreover, several schemes to read the cavity and the atomic states are currently available [38, 39, 47] (or under investigation [48]). The main task would be finding a way to modulate periodically the atomic transition frequency with a stable modulation frequency  $\eta \sim 10$  GHz, what is also

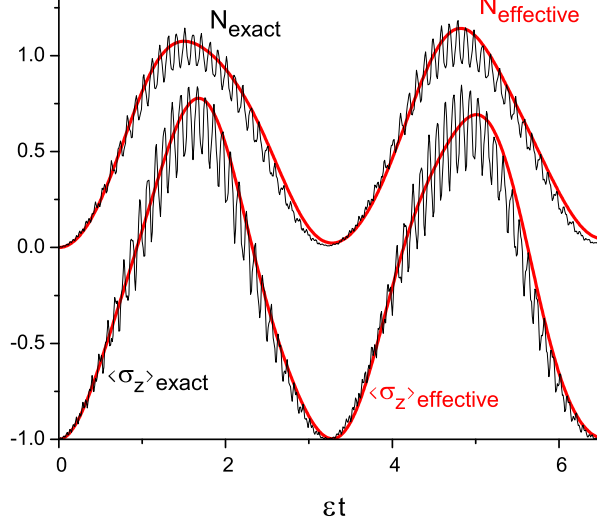


FIG. 5: The mean number of created photons  $N$  and atomic population inversion  $\langle s_z \rangle$  obtained numerically for the exact [equation (3)] and effective [equation (46)] Hamiltonians for the resonance shift  $\xi = -\delta_0$ . The exact  $N$  and  $\langle \sigma_z \rangle$  show rapid oscillations, while the effective ones are smooth.

within an experimental reach [37]. One could also use this scheme to couple  $M$  identical qubits (e.g. superconducting 2-level atoms [37, 43] or a cloud of polar molecules [30, 31]) to the same cavity mode and modulate the frequency of  $M$  atoms simultaneously, since in this case the effective coupling is increased to  $\sqrt{M}g_0$ .

One important point we did not analyze here is the dissipation and decoherence of both the artificial atom and the cavity due to the noisy solid state environment [48, 67]. Recent experiments achieved experimental values  $\{\kappa/\omega < 10^{-4}, \gamma/\omega < 10^{-3}, \gamma_{ph}/\omega < 10^{-3}\}$  [39], where  $\kappa$  is the cavity decay rate,  $\gamma$  is the atomic decay rate and  $\gamma_{ph}$  is the atomic pure dephasing rate. To deal with dissipation in a qualitative manner, we compare the rates of the photon generation from vacuum for each resonance to the dissipation rates. We take the current experimental value of the coupling constant  $g_0/\omega \approx 2 \cdot 10^{-2}$  [39] and assume  $\epsilon/\omega \sim \Delta_-/\omega \sim 10^{-1}$  to make the estimative. The photon creation rate for the first order DCE resonance is roughly  $|\delta\theta|/\omega \sim 10^{-4}$  [equation (35)], and for the first order AJC resonance is roughly  $g_0|\theta|/\omega \sim 10^{-3}$  [equation (18)]. Both these values are larger than the dissipation and decoherence rates (or of the same order of magnitude). Therefore, the photon creation due to modulation of  $\Omega(t)$  or  $g_0(t)$  seems possible in the future.

## VII. A GLANCE AT NONPERIODIC MODULATION

Let us now consider that the coupling parameter  $g(t)$  has a bichromatic external modulation

$$g(t) = g_0 + 2\epsilon \sin[(\Delta_+ - 2\xi)t] + 2\epsilon_- \sin[(\Delta_- - 2\xi_-)t], \quad (42)$$

where  $g_0$  is the bare coupling parameter,  $|\epsilon|, |\epsilon_-| \ll g_0$  are small modulation amplitudes and  $\xi, \xi_-$  are the ‘resonance shifts’. Here  $\Delta_{\pm}$  is given by equation (10) with  $c_0 = 0$  (i.e.,  $\Delta_{\pm} = \Omega \pm \omega$ ) and we assume  $\Delta_- > 0$ . The system Hamiltonian is given by equation (3) with time-dependent  $g(t)$  and constant  $\omega$  and  $\Omega$ . In the dispersive regime, we obtain the effective Hamiltonian

$$H_{eff} \simeq \delta(\hat{n} + 1/2)\sigma_z + (i\epsilon e^{2i\xi t} a^\dagger \sigma_+ + i\epsilon_- e^{2i\xi_- t} a \sigma_+ + h.c.). \quad (43)$$

Performing the unitary time-dependent transformation

$$U_3 = \exp\{i[(\xi + \xi_-)\sigma_z/2 + (\xi - \xi_-)\hat{n}]t\} \quad (44)$$

we get the time-independent Hamiltonian combining the ‘rotating’ and ‘anti-rotating’ terms with adjustable couplings

$$\begin{aligned} H_{np} &\simeq U_3^{-1} H_{eff} U_3 - iU_3^{-1} \frac{\partial U_3}{\partial t} \\ &= \frac{\xi + \xi_- + \delta(1 + 2\hat{n})}{2} \sigma_z + (\xi - \xi_-) \hat{n} + (i\varepsilon a^\dagger \sigma_+ + i\varepsilon_- a \sigma_+ + h.c.). \end{aligned} \quad (45)$$

We take equal resonance shifts in order to cancel the second term in (45),  $\xi = \xi_-$ , so for  $\varepsilon_- = 0$  ( $\varepsilon = 0$ ) we obtain the effective Anti-Jaynes-Cummings (Jaynes-Cummings) Hamiltonian. A more interesting regime occurs when both  $\varepsilon$  and  $\varepsilon_-$  are different from zero. For  $\varepsilon = \varepsilon_-$  we obtain

$$H_+ \simeq \frac{2\xi + \delta(1 + 2\hat{n})}{2} \sigma_z + i\varepsilon(a + a^\dagger)(\sigma_+ - \sigma_-), \quad (46)$$

while for  $\varepsilon = -\varepsilon_-$  we get (46) with the last term replaced by  $i\varepsilon(a - a^\dagger)(\sigma_+ + \sigma_-)$ . The Hamiltonian (46) cannot be integrated exactly, so below we solve it numerically and compare the results to the ones obtained using the initial Rabi Hamiltonian (3).

To obtain photon creation from the initial vacuum state  $|g, 0\rangle$ , we have to make the exponent multiplying  $\sigma_z$  in (46) as small as possible by adjusting the resonance shift  $\xi$ . In figure 5 we show the mean number of created photons  $N$  and the population inversion  $\langle s_z \rangle$  as function of dimensionless time  $\varepsilon t$  for  $\varepsilon = \varepsilon_-$  and  $\xi = -\delta_0$ , calculated numerically for the initial Hamiltonian (3) and the effective Hamiltonian (46) using the parameters  $\Omega/\omega = 1.3$ ,  $g_0/\omega = 5 \cdot 10^{-2}$  and  $\varepsilon/\omega = 5 \cdot 10^{-3}$ . One can see that the effective Hamiltonian  $H_+$  describes well the exact dynamics, and there is a quasi-periodic generation of a few photons, together with the atomic excitation. Qualitatively, this occurs because for initial times the Hamiltonian (46) becomes

$$H_+ \simeq -\sqrt{2}\varepsilon x \sigma_y, \quad (47)$$

and the photons are generated from vacuum quadratically in time. However, after  $\sim 1$  photons have been created, the exponent multiplying  $\sigma_z$  in (46) becomes large, so the photon creation process goes out of resonance and it is interrupted.

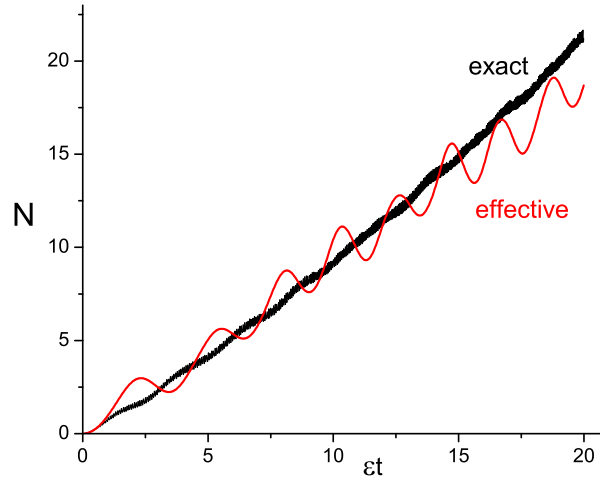


FIG. 6: The mean number of created photons  $N$  obtained numerically for the exact [equation (3)] and effective [equation (46)] Hamiltonians for the resonance shift  $\xi = \tilde{\xi}(t)$  [equation (48)]. The effective  $N$  shows slow oscillations, while the exact one does not.

To create a large number of photons from vacuum, we can adopt an ‘active’ approach, by which the resonance shift  $\xi$  is adjusted *adiabatically* as function of time, so the effective Hamiltonian (45) is valid. In this way, we continuously adjust the resonance shift to the number of photons in the cavity, provided we choose an appropriate functional form

of  $\xi$ . In figure 6 we show the mean number of created photons  $N$  from the initial state  $|g, 0\rangle$  for the Rabi Hamiltonian (3) and the effective Hamiltonian (46), using the parameters  $\Omega/\omega = 1.4$ ,  $g_0/\omega = 5 \cdot 10^{-2}$ ,  $\varepsilon/\omega = 5 \cdot 10^{-3}$  and setting

$$\xi = \tilde{\xi}(t) = -(\delta_0 - 3g_0^2/\Delta_+) (1/2 + \varepsilon t). \quad (48)$$

One can see that a significant amount of photons can be generated from vacuum, provided the resonance shift is adjusted adiabatically, and the effective Hamiltonian  $H_+$  describes well the exact dynamics.

Finally, notice that these results also hold if, instead of the coupling parameter  $g$ , one modulates the atomic transition frequency  $\Omega$ , or both  $g$  and  $\Omega$  simultaneously, one with frequency  $\sim \Delta_+$ , and another with  $\sim \Delta_-$ .

## VIII. CONCLUSIONS

In conclusion, we studied the nonstationary solid state cavity QED system in which the atomic transition frequency or the atom-cavity coupling have a small periodic time modulation, prescribed externally. We showed that in the dispersive regime and under the resonant modulations, the Rabi Hamiltonian (which describes the system dynamics) can be significantly simplified, resulting in three different regimes that can be described by the Anti-Jaynes-Cummings, Jaynes-Cummings or the dynamical Casimir effect Hamiltonians. Moreover, in the resonant atom-cavity regime, entangled states with two photons can be created from the vacuum state  $|g, 0\rangle$  under the corresponding resonance, analogously to the dynamical Casimir effect in a vibrating cavity containing a resonant two-level atom.

We also showed that the photon generation from vacuum occurs for a small nonperiodic time modulation of the atom-cavity coupling, the atomic transition frequency, or both in circuit QED. We deduced an effective Hamiltonian for the bichromatic modulation in the dispersive regime, and demonstrated that it describes well the exact dynamics. Numerical simulations confirmed that several photons can be generated from vacuum provided the modulation frequencies are fine tuned adiabatically.

This study illustrates the importance of the anti-rotating terms in the Rabi Hamiltonian, ignored in the Jaynes-Cummings model – here this term is responsible for photon generation from vacuum and field amplification. Moreover, one could engineer effective interactions in nonstationary circuit QED by means of modulating the system parameters. As applications, this scheme can be used to verify photon creation from vacuum in nonstationary circuit QED due to an analog of the dynamical Casimir effect using a single atom, as well as off-resonant population transfer between the states  $\{|g, n\rangle, |e, n \pm 1\rangle\}$  and generation of entangled states with several photons.

## Acknowledgments

Work supported by FAPESP (SP, Brazil, contract No. 04/13705-3), ITAMP (at Harvard University and Smithsonian Astrophysical Observatory) and (partially) by National Science Foundation.

- 
- [1] Sassaroli E, Srivastava Y N and Widom A 1994 Photon production by the dynamical Casimir effect *Phys. Rev. A* **50** 1027
  - [2] Dalvit D A R and Mazzitelli F D 1998 Renormalization-group approach to the dynamical Casimir effect *Phys. Rev. A* **57** 2113
  - [3] Dodonov V V 1998 Dynamical Casimir effect in a nondegenerate cavity with losses and detuning *Phys. Rev. A* **58** 4147
  - [4] Law C K 1994 Resonance response of the quantum vacuum to an oscillating boundary *Phys. Rev. Lett.* **73** 1931
  - [5] Law C K 1995 Interaction between a moving mirror and radiation pressure: A Hamiltonian formulation *Phys. Rev. A* **51** 2537
  - [6] Yablonovitch E 1989 Accelerating reference frame for electromagnetic waves in a rapidly growing plasma: Unruh–Davies–Fulling–De Witt radiation and the nonadiabatic Casimir effect *Phys. Rev. Lett.* **62** 1742
  - [7] Schwinger J 1993 Casimir light: a glimpse *Proc. Nat. Acad. Sci. USA* **90** 958
  - [8] Dodonov V V, Klimov A B and Nikonov D E 1993 Quantum phenomena in nonstationary media *Phys. Rev. A* **47** 4422
  - [9] Johnston H and Sarkar S 1995 Moving mirrors and time-varying dielectrics *Phys. Rev. A* **51** 4109
  - [10] Barton G, Dodonov V V and Man'ko V I 2005 The nonstationary Casimir effect and quantum systems with moving boundaries *J. Opt. B: Quant. Semiclass. Opt.* **7** S1
  - [11] Dodonov V V 2001 Nonstationary Casimir effect and analytical solutions for quantum fields in cavities with moving boundaries *Modern Nonlinear Optics (Advances in Chemical Physics Series vol 119, part 1)* ed M W Evans (New York: Wiley) pp 309–94 (Preprint arXiv: quant-ph/0106081)
  - [12] Dodonov V V and Dodonov A V 2005 Quantum harmonic oscillator and nonstationary Casimir effect *J. Rus. Las. Res.* **26** 445

- [13] Dodonov A V and Dodonov V V 2005 Resonance generation of photons from vacuum in cavities due to strong periodical changes of conductivity in a thin semiconductor layer *J. Opt. B: Quant. Semiclass. Opt.* **7** S47
- [14] Dodonov V V and Dodonov A V 2006 The nonstationary Casimir effect in a cavity with periodical time-dependent conductivity of a semiconductor mirror *J. Phys. A: Math. and General* **39** 6271
- [15] Kim W-J, Brownell J H Onofrio R 2006 Detectability of dissipative motion in quantum vacuum via superradiance *Phys. Rev. Lett.* **96** 200402
- [16] Segev E, Abdo B, Shtempluck O, Buks E and Yurke B 2007 Prospects of employing superconducting stripline resonators for studying the dynamical Casimir effect experimentally *Phys. Lett. A* **370** 202
- [17] De Liberato S, Ciuti C and Carusotto I 2007 Quantum vacuum radiation spectra from a semiconductor microcavity with a time-modulated vacuum Rabi frequency *Phys. Rev. Lett.* **98** 103602
- [18] Carusotto I, Antezza M, Bariani F, De Liberato S and Ciuti C 2008 Optical properties of atomic Mott insulators: From slow light to dynamical Casimir effects *Phys. Rev. A* **77** 063621
- [19] Braggio C, Bressi G, Carugno G, Lombardi A, Palmieri A, Ruoso G and Zanello D 2004 Semiconductor microwave mirror for a measurement of the dynamical Casimir effect *Rev. Sci. Instr.* **75** 4967
- [20] Braggio C, Bressi G, Carugno G, Del Noce C, Galeazzi G, Lombardi A, Palmieri A, Ruoso G and Zanello D 2005 A novel experimental approach for the detection of the dynamical Casimir effect *Europhys. Lett.* **70** 754
- [21] Agnesi A, Braggio C, Bressi G, Carugno G, Galeazzi G, Pirzio F, Reali G, Ruoso G Zanello D 2008 MIR status report: an experiment for the measurement of the dynamical Casimir effect *J. Phys. A: Math. Theor.* **41** 164024
- [22] Raimond J, Brune M and Haroche S 2001 Manipulating quantum entanglement with atoms and photons in a cavity *Rev. Mod. Phys.* **73** 565
- [23] Mabuchi H and Doherty A C 2002 Cavity quantum electrodynamics: Coherence in context *Science* **298** 1372
- [24] Reithmaier J P, Sek G, Löffler A, Hofmann C, Kuhn S, Reitzenstein S, Keldysh L V, Kulakovskii V D, Reinecke T L and Forchel A 2004 Strong coupling in a single quantum dot-semiconductor microcavity system *Nature* **432** 197
- [25] Yoshie T, Scherer A, Hendrickson J, Khitrova G, Gibbs H M, Rupper G, Ell C, Shchekin O B and Deppe D G 2004 Vacuum Rabi splitting with a single quantum dot in a photonic crystal nanocavity *Nature* **432** 200
- [26] Englund D, Faraon A, Fushman I, Stoltz N, Petroff P and Vuckovic J 2007 Controlling cavity reflectivity with a single quantum dot *Nature* **450** 857
- [27] Fushman I, Englund D, Faraon A, Stoltz N, Petroff P and Vuckovic J 2008 Controlled phase shifts with a single quantum dot *Science* **320** 769
- [28] Badolato A, Hennessy K, Atature M, Dreiser J, Hu E, Petroff P M and Imamoglu A 2005 Deterministic coupling of single quantum dots to single nanocavity modes *Science* **308** 1158
- [29] Hennessy K, Badolato A, Winger M, Gerace D, Atature M, Gulde S, Falt S, Hu E L and Imamoglu A 2007 Quantum nature of a strongly coupled single quantum dot-cavity system *Nature* **445** 896
- [30] Andre A, Demille D, Doyle J M, Lukin M D, Maxwell S E, Rabl P, Schoelkopf R J and Zoller P 2006 A coherent all-electrical interface between polar molecules and mesoscopic superconducting resonators *Nature Physics* **2** 636
- [31] Rabl P, DeMille D, Doyle J M, Lukin M D, Schoelkopf R J and Zoller P 2006 Hybrid quantum processors: Molecular ensembles as Quantum memory for solid state circuits *Phys. Rev. Lett.* **97** 033003
- [32] Chiorescu I, Bertet P, Semba K, Nakamura Y, Harmans C J P M and Mooij J E 2004 Coherent dynamics of a flux qubit coupled to a harmonic oscillator *Nature* **431** 159
- [33] Wallraff A, Schuster D I, Blais A, Frunzio L, Huang R S, Majer J, Kumar S, Girvin S M and Schoelkopf R J 2004 Strong coupling of a single photon to a superconducting qubit using circuit quantum electrodynamics *Nature* **431** 162
- [34] Johansson J, Saito S, Meno T, Nakano H, Ueda M, Semba K and Takayanagi H 2006 Vacuum Rabi oscillations in a macroscopic superconducting qubit LC oscillator system *Phys. Rev. Lett.* **96** 127006
- [35] Zagoskin A and Blais A 2007 Superconducting qubits *Phys. Can.* **63** 215 (Preprint arXiv: 0805.0164)
- [36] Sandberg M, Wilson C M, Persson F, Johansson G, Shumeiko V, Duty T and Delsing P 2008 In-situ frequency tuning of photons stored in a high Q microwave cavity *Preprint arXiv: 0801.2479*.
- [37] Sillanpää M A, Park J I and Simmonds R W 2007 Coherent quantum state storage and transfer between two phase qubits via a resonant cavity *Nature* **449** 438
- [38] Blais A, Huang R-S, Wallraff A, Girvin S M and Schoelkopf R J 2004 Cavity quantum electrodynamics for superconducting electrical circuits: An architecture for quantum computation *Phys. Rev. A* **69** 062320
- [39] Schuster D I, Houck A A, Schreier J A, Wallraff A, Gambetta J M, Blais A, Frunzio L, Majer J, Johnson B, Devoret M H, Girvin S M and Schoelkopf R J 2007 Resolving photon number states in a superconducting circuit *Nature* **445** 515
- [40] Houck A A, Schuster D I, Gambetta J M, Schreier J A, Johnson B R, Chow J M, Frunzio L, Majer J, Devoret M H, Girvin S M and Schoelkopf R J 2007 Generating single microwave photons in a circuit *Nature* **449** 328
- [41] Astafiev O, Inomata K, Niskanen A O, Yamamoto T, Pashkin Yu A, Nakamura Y and Tsai J S 2007 Single artificial-atom lasing *Nature* **449** 588
- [42] Hofheinz M, Weig E M, Ansmann M, Bialczak R C, Lucero E, Neeley M, O'Connell A D, Wang H, Martinis J M and Cleland A N 2008 Generation of Fock states in a superconducting quantum circuit *Nature* **454** 310
- [43] Majer J, Chow J M, Gambetta J M, Koch J, Johnson B R, Schreier J A, Frunzio L, Schuster D I, Houck A A, Wallraff A, Blais A, Devoret M H, Girvin S M and Schoelkopf R J 2007 Coupling superconducting qubits via a cavity bus *Nature* **449** 443
- [44] Schuster D I, Wallraff A, Blais A, Frunzio L, Huang R-S, Majer J, Girvin S M and Schoelkopf R J 2005 ac Stark shift and dephasing of a superconducting qubit strongly coupled to a cavity field *Phys. Rev. Lett.* **94** 123602
- [45] Gambetta J, Blais A, Schuster D I, Wallraff A, Frunzio L, Majer J, Devoret M H, Girvin S M and Schoelkopf R J 2006

- Qubit-photon interactions in a cavity: Measurement-induced dephasing and number splitting *Phys. Rev. A* **74** 042318
- [46] Gambetta J, Braff W A, Wallraff A, Girvin S M and Schoelkopf R J 2007 Protocols for optimal readout of qubits using a continuous quantum nondemolition measurement *Phys. Rev. A* **76** 012325
- [47] Wallraff A, Schuster D I, Blais A, Frunzio L, Majer J, Devoret M H, Girvin S M and Schoelkopf R J 2005 Approaching unit visibility for control of a Superconducting qubit with dispersive readout *Phys. Rev. Lett.* **95** 060501
- [48] Blais A, Gambetta J, Wallraff A, Schuster D I, Girvin S M, Devoret M H and Schoelkopf R J 2007 Quantum-information processing with circuit quantum electrodynamics *Phys. Rev. A* **75** 032329
- [49] Leek P J, Fink J M, Blais A, Bianchetti R, Göppl M, Gambetta J M, Schuster D I, Frunzio L, Schoelkopf R J and Wallraff A 2007 Observation of Berry's phase in a solid-state qubit *Science* **318** 1889
- [50] Saito K, Wubs M, Kohler S, Hänggi P and Kayanuma Y 2006 Quantum state preparation in circuit QED via Landau-Zener tunneling *Europhys. Lett.* **76** 22
- [51] Wubs M, Kohler S and Hanggi P 2007 Entanglement creation in circuit QED via Landau-Zener sweeps *Physica E - Low-Dim. Syst. Nanostr.* **40** 187
- [52] Ciuti C and Carusotto I 2007 On the ultrastrong vacuum Rabi coupling of an intersubband transition in a semiconductor microcavity *J. Appl. Phys.* **101** 081709
- [53] Ciuti C, Bastard G and Carusotto I 2005 Quantum vacuum properties of the intersubband cavity polariton field *Phys. Rev. B* **72** 115303
- [54] Takashima K, Hatakenaka N, Kurihara S and Zeilinger A 2008 Nonstationary boundary effect for a quantum flux in superconducting nanocircuits *J. Phys. A: Math. Theor.* **41** 164036
- [55] Dodonov A V, Céleri L C, Pascoal F, Lukin M D and Yelin S F 2008 Photon generation from vacuum in non-stationary circuit QED *Preprint* arXiv: 0806.4035
- [56] Hauss J, Fedorov A, André S, Brosco V, Hutter C, Kothari R, Yeshwanth S, Shnirman A and Schön G 2008 Dissipation in circuit quantum electrodynamics: lasing and cooling of a low-frequency oscillator *New J. Phys.* **10** 095018
- [57] Schleich W P 2001 *Quantum Optics in Phase Space* (Wiley-VCH Verlag, Berlin)
- [58] Fink J M, Göppl M, Baur M, Bianchetti R, Leek P J, Blais A and Wallraff A 2008 Climbing the Jaynes-Cummings ladder and observing its  $\sqrt{n}$  nonlinearity in a cavity QED system *Nature* **454** 315
- [59] Schuster I, Kubanek A, Fuhrmanek A, Puppe T, Pinkse P W H, Murr K and Rempe G 2008 Nonlinear spectroscopy of photons bound to one atom *Nature Physics* **4** 382
- [60] Bishop L S, Chow J M, Koch J, Houck A A, Devoret M H, Thuneberg E, Girvin S M and Schoelkopf R J 2008 Nonlinear response of the vacuum Rabi resonance *Preprint* arXiv: 0807.2882
- [61] Werlang T, Dodonov A V, Duzzioni E I and Villas-Bôas C J 2008 Rabi model beyond the rotating-wave approximation: Generation of photons from vacuum through decoherence *Phys. Rev. A* **78** 053805
- [62] Dodonov V V (1995 Photon creation and excitation of a detector in a cavity with a resonantly vibrating wall *Phys. Lett. A* **207** 126
- [63] Fedotov A M, Narozhny N B and Lozovik Y E 2000 'Shaking' of an atom in a non-stationary cavity *Phys. Lett. A* **274** 213
- [64] Narozhny N B, Fedotov A M and Lozovik Y E 2001 Dynamical Lamb effect versus dynamical Casimir effect *Phys. Rev. A* **64** 053807
- [65] Narozhny N B, Fedotov A M and Lozovik Y E 2003 Dynamical Casimir and Lamb effects and entangled photon states *Las. Phys.* **13** 298
- [66] Klimov A B and Chumakov S M 2008 *A Group Theoretical Approach to Quantum Optics* (Wiley-VCH, Berlin)
- [67] Houck A A, Schreier J A, Johnson B R, Chow J M, Koch J, Gambetta J M, Schuster D I, Frunzio L, Devoret M H, Girvin S M and Schoelkopf R J 2008 Controlling the spontaneous emission of a superconducting transmon qubit *Phys. Rev. Lett.* **101** 080502
- [68] If initially the atom is in the superpositions of states  $|g\rangle$  and  $|e\rangle$ , we can choose any of the signs to obtain photon generation. However, the photon generation is optimized if initially the atom is exactly in  $|g\rangle$  or  $|e\rangle$ .
- [69] One could adjust the resonance shift adiabatically in time to enhance the resonance.